PHYSICAL REVIEW B **79**, 224302 (2009)

Observation of mass transport through solid ^{4}He

M. W. Ray and R. B. Hallock
Department of Physics, Laboratory for Low Temperature Physics, University of Massachusetts, Amherst, Massachusetts 01003, USA
(Received 10 February 2009; revised manuscript received 23 April 2009; published 16 June 2009)

By use of an experimental design that provides for superfluid helium in contact with bulk hcp ^{4}He off the melting curve, we have observed the dc transport of mass through a cell filled with solid ^{4}He in the hcp region of the phase diagram. Flow, which shows characteristics of a superflow, is seen to be independent of the method used to grow the solid but depends on pressure and temperature. The temperature dependence suggests the possibility of hysteresis.

DOI: 10.1103/PhysRevB.79.224302 PACS number(s): 67.80.bd, 67.90.+z

I. INTRODUCTION

The possibility of a superfluid solid, or a so-called[1,2] supersolid phase, in solid ^{4}He has been discussed for many years,[3–7] but until recently no evidence for such a state had been observed experimentally. In 2004, motivated by the experiments of Ho *et al.*,[8] Kim and Chan[9–12] reported a reduction in the resonant period of a torsion oscillator filled with solid hcp helium. Although their interpretation that this nonclassical rotational inertia (NCRI), as it was called, was evidence of a supersolid state remains controversial, it renewed intense interest in the subject. Since the Kim and Chan results, there have been several other[13–16] torsion-oscillator experiments performed confirming the earlier results but showing a considerable range of NCRI values. Rittner and Reppy[15] observed a sample history dependence with large "superfluid" fractions (~20%) measured in quench-cooled samples that had small macroscopic dimensions and saw reductions in the "superfluid" fractions that depended on how much the sample had annealed. Aoki *et al.*[16] observed a frequency-dependent NCRI and studied "limiting velocities," showing a complicated dependence on sample history. Day and Beamish[17] studied the shear modulus of solid ^{4}He and saw that it increased at approximately the same temperature as the observed onset of substantial changes in the NCRI. This surprising result was explained by the depinning of dislocations embedded in the solid. Because it showed a dependence on temperature and ^{3}He concentration similar to that in torsion-oscillator experiments, it was thought that the behavior of the shear modulus might be closely related to the NCRI results.

Any superfluid phase should support a frictionless mass transport. Therefore, if this nonclassical rotational inertia is indeed evidence of supersolidity in helium, then a superflow should be possible. Several experiments have investigated this directly, and all found no evidence of such a transport of mass. Greywall[18] saw no flow when he attempted to push solid helium through 200-μm-diameter capillaries. A somewhat similar experiment was performed recently by Day *et al.*[19] in which they tried to push helium through the small (7 nm) pores of Vycor glass. An experiment by Day and Beamish[20] extended the results to glass-capillary arrays with 25-μm-diameter pores. Recent work by Rittner *et al.*[21] searched for flow in thin quench-cooled samples. No evidence for flow was seen in those experiments. Bonfait *et al.*[22] took a different approach. They grew solid helium in a concentric, cylindrical, U-tube-like geometry on the melting curve with liquid helium on either side. They then attempted to observe equilibration in the different levels of the solid free surface on the two sides of the U tube; no equilibration took place. A very similar approach was taken by Sasaki *et al.*[23,24] with the inclusion of a window to allow direct visual images of the solid sample. The measurements showed that the positions of the solid free surfaces shifted, and this was interpreted as being due to mass flow through the solid along grain boundaries which were visually identifiable in the sample;[23] when grain boundaries disappeared, so did the observable flow. Later analysis, however, showed that flow was most probably occurring along liquid channels that exist where a grain boundary meets the wall of the cell or where grain boundaries intersect.[24,25]

It is now believed theoretically that the observed NCRI behavior of the solid helium is likely due to disorder and is not an intrinsic property of a solid helium crystal. In fact it has been shown theoretically that the original interpretations of the torsion-oscillator results as a Bose-Eintstein condensate of vacancies in the crystal are likely wrong[26] and that a perfect vacancy-free solid helium crystal cannot become a supersolid.[27–29] Simulations have shown that a frictionless flow of mass through solid ^{4}He can occur through defects in the solid, such as grain boundaries[30] and dislocations.[31] Simulations have also shown that under certain conditions a glassy state[32,33] of solid helium, a "superglass,"[34] may allow for a superflow.[35] However, whether or not these defects can account for the observed NCRI has not yet been shown. In particular, the understanding of superfluid fractions as large as 20% in quench-cooled samples remains a mystery.

We have previously briefly reported on an experiment in which we were able to induce mass flow through solid helium.[36,37] This report provides additional data and more extensive details of our work. Our approach is conceptually different from the previous flow experiments of Greywall[18] and Beamish *et al.*[19,20] In our approach we inject atoms into the solid rather than apply a mechanical force to squeeze the lattice. A key difference between our experiments and those of Sasaki *et al.*,[23] who observed a shift in the relative positions of solid-liquid interfaces, is that we have employed the properties of liquid helium in a confined geometry (Vycor) to create a liquid-solid interface that is not on the bulk melting curve. We are thus able to apply a chemical-potential differ-

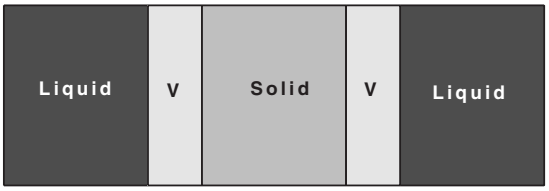

FIG. 1. Conceptual representation of the experiment showing the sandwich-like geometry with three chambers, each pair of which is separated by a region of liquid helium-filled porous Vycor glass, V. In operation a temperature difference is applied across each of the regions of Vycor, which keeps the liquid reservoirs from freezing.

ence directly across the solid without the application of mechanical pressure to the lattice. This approach allows us to perform zero-frequency flow experiments by injecting helium at low temperatures and at pressures in excess of the bulk solidification pressure, (~25 bar). In Sec. II we describe the apparatus we have developed and explain our procedures. In Sec. III we discuss various methods we have employed for the growth of our solid helium samples. In Sec. IV we present our results. Section V discusses those results, including various possible alternate explanations for our observations. In Sec. VI we summarize our conclusions. We also include Appendices of atypical observations and include tables, which provide details relevant to the data sets.

II. EXPERIMENTAL DESIGN

The concept of our experiment is very simple, and the basic idea is shown in Fig. 1. Three chambers are separated from each other by porous Vycor glass. The center chamber contains the solid hcp helium sample, while the outer chambers and Vycor contain liquid helium. With the pressure of the outside reservoirs, and hence in the Vycor, below ~37 bar the helium inside the Vycor will remain a liquid (Fig. 2) due to the confined geometry provided by the pores.[38–40] Thus, by imposing a temperature gradient across

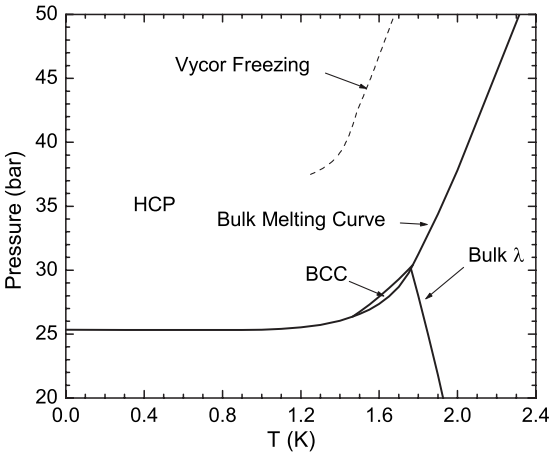

FIG. 2. Phase diagram of helium showing the melting curve for helium inside of porous Vycor glass, adapted from previous work (Refs. 38–40).

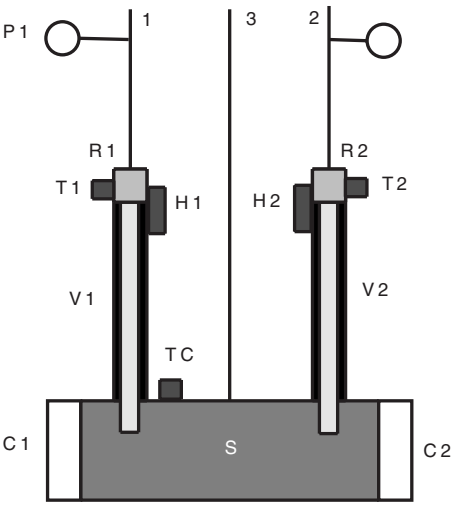

FIG. 3. Schematic diagram of the cell used for flow experiments. Three fill lines lead to the cell, two go to liquid reservoirs R1 and R2 above the Vycor rods V1 and V2. The third one leads directly to the solid chamber, S. Two capacitance pressure gauges, C1 and C2, sit on either side of the cell for *in situ* pressure measurements. Pressures in the Vycor lines (1 and 2) are read by pressure transducers outside of the cryostat. Each reservoir has a heater, H1 and H2, which prevents the liquid in it from freezing, and the reservoir temperatures are read by carbon resistance thermometers T1 and T2. The cell temperature is recorded by a third carbon resistance thermometer, TC. The cell thermometer reading, denoted as TC, provides the temperature of the sample, *T*.

the Vycor so that the liquid in the reservoirs does not freeze, we can maintain liquid helium in contact with solid helium with the bulk solid off the melting curve at a given temperature. To perform the experiment we simply create a chemical-potential difference between the two liquid chambers by, say, injecting helium atoms into one side to raise its pressure, a process we have termed as a "push" or an "injection." Alternatively, we can lower the pressure on one side, which we have termed a "pull" or "withdrawal." We then monitor the pressure in the other fill line for a response; if the two pressures come toward equilibrium then mass had to have moved through the cell that contains solid ^{4}He.

The cell designed for these flow experiments is shown schematically in Fig. 3. Three stainless-steel capillaries lead to the cell. Two of them (numbered 1 and 2) lead to the liquid reservoirs, R1 and R2, which are at the top of the Vycor rods, which have a diameter of 1.5 mm. These two capillaries are heat sunk only at 4 K, which allows us to keep solid helium from forming in them. Capillary 3, heat sunk at 1 K, leads directly to the solid chamber S, which is cylindrical in shape with a diameter of 6.35 mm. Capillary 3 was mainly used to aid in the initial fill and final evacuation of the cell since under some conditions, the flow of helium through the pores of the Vycor was slow. The Vycor rods are epoxied into thin (0.8 mm wall thickness) stainless-steel tubes using Stycast 2850 FT. The centers of the Vycor rods are positioned 20.6 mm apart; they extend approximately 6 mm into S and each provides 0.30 cm^2 of macroscopic surface area of contact between the Vycor and the bulk solid in the sample chamber. Capacitance pressure gauges of the

Straty and Adams type[41] are attached to each end of the cell to measure the pressure of the solid *in situ*. This arrangement also allows us to measure any pressure gradients in the solid that may appear, an issue that we will return to later. There are two carbon resistance thermometers on each of S, R1 and R2; one for temperature control and one for recording the temperature (the temperature controlling thermometers are not shown in Fig. 3). Two heaters, H1 and H2, were used to maintain a temperature gradient and ensured that the liquid in R1 and R2 did not freeze. The whole solid chamber, S, is bolted to a copper plate which is attached to the mixing chamber of a dilution refrigerator by six 6.35-mm-diameter copper rods.

The heat flow down the Vycor rods was higher than we anticipated and is an issue that we hope to resolve with the next generation of the apparatus. The stainless-steel rods that house the Vycor were designed to keep the heat flow from the warmer liquid reservoirs to the cold solid chamber to a low level. We estimated that with no helium in the Vycor, the cell at 100 mK, and the Vycor top at 1.7 K, the heat flow to the cell should be no more than ≈ 20 μW. When designing this experiment it was our belief that liquid helium should not contribute much to the thermal conductivity of the Vycor and stainless-steel combination. Ideally, the small pore size of the Vycor should act as a superleak allowing superfluid to pass (which provides for a fountain effect) but blocking the flow of normal fluid, thus preventing thermal counterflow. Unfortunately the observed heat load on our mixing chamber with helium in the apparatus was larger than expected, and thus our lowest temperature with helium in the cell was limited to ~ 300 mK, depending on the pressure.

This problem of the heat load could be attributed to one or more causes. For instance, a hole through the Vycor that is several times larger than the nominal pore size or a break in the epoxy that gives normal fluid a path to move around the Vycor could enhance the effective thermal conductivity. Subsequent to some of our measurements we were advised that Vycor rods might have an axial imperfection in which the Vycor structure differs from the usual structure. Evidence for this was first reported by Wilson *et al.*[42] Indeed, careful subsequent inspection of several samples from our batch of Vycor rods revealed a small axially symmetric imperfection (≈ 25 μm in diameter) that appears to continue down the entire length of the inspected rods. It is possible that this imperfection is found only in Vycor rods;[43] plates may have a similar imperfection but of planar geometry.[44] The elevated heat conduction could also be due to fluid shorts along the side of the Vycor. For instance, the epoxy might crack, possibly due to differing thermal-expansion coefficients, which might allow a path big enough for some limited thermal counterflow to occur. The thermal-expansion coefficient of Stycast 2850 is 1.5 times greater than stainless steel[45]; Vycor, if it is like many glasses,[45] should have an expansion coefficient smaller than stainless steel.

Despite the fact that the heat load has prevented us from reaching the most desirable lower temperatures, it does not affect the central conclusion of our experiment that we have observed a flux of atoms through solid helium housed in our sample cell. With regard to the effect of the Vycor, any bulk liquid-helium path around or in the Vycor should freeze in the low-temperature region of the Vycor once the pressure goes much above the bulk melting pressure. Although our current lowest temperature achieved is higher than the temperature at which substantial changes in NCRI set in for the torsion-oscillator experiments ($\sim 60-80$ mK), we have nonetheless been able to grow solid helium, learn about the behavior of this system, and make interesting observations.

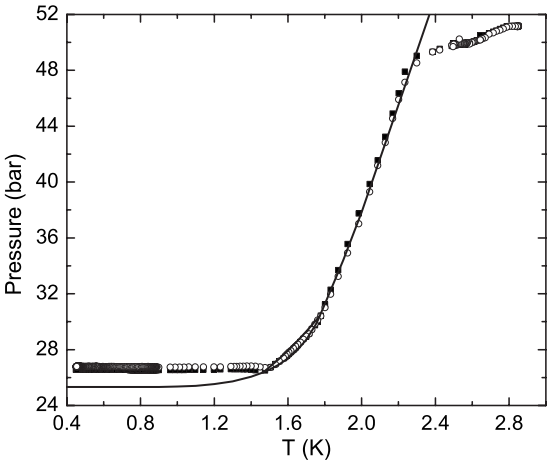

FIG. 4. Solid growth by the blocked capillary technique. The two sets of symbols represent data from the two pressure gauges on the cell, C1 and C2, and the solid line is the bulk-helium melting curve.

III. SAMPLE GROWTH

There are several different techniques that can be used to grow solid helium crystals. Each one is likely to create solid ^{4}He samples of different quality, with differing numbers of defects. Techniques that minimize stresses as the crystals grow are expected to result in higher quality samples. Since the torsion-oscillator results are now thought to be caused by the disorder in the solid, it would be interesting to study a variety of growth techniques in our experiments.

The most widely used growth technique is the blocked capillary method. In this method a plug of solid helium is formed in the fill line, and the cell is cooled with a constant number of atoms present. During solid helium growth the pressure and temperature change substantially as the growing solid follows the melting curve, which causes strain in the solid. It is for this reason that blocked capillary growth is thought to produce more disordered crystals. Furthermore, crystals grown this way may pass through the bcc region of the phase diagram, which is also believed to adversely effect the crystal quality.[46] Our cell allows us to grow crystals using a slightly modified blocked capillary technique. The 1 K heat sink on line 3 allows us to form a solid helium plug in that capillary. As we will describe, we could limit the liquid from entering the cell from lines 1 and 2 since while the cell is on the melting curve the lines are filled entirely with normal fluid and we control the pressure in the fill lines.

Figure 4 shows a typical trajectory of the cell for blocked capillary growth. Starting near 51 bar and 2.8 K, we freeze the helium in line 3 and start cooling the cell. The intersec-

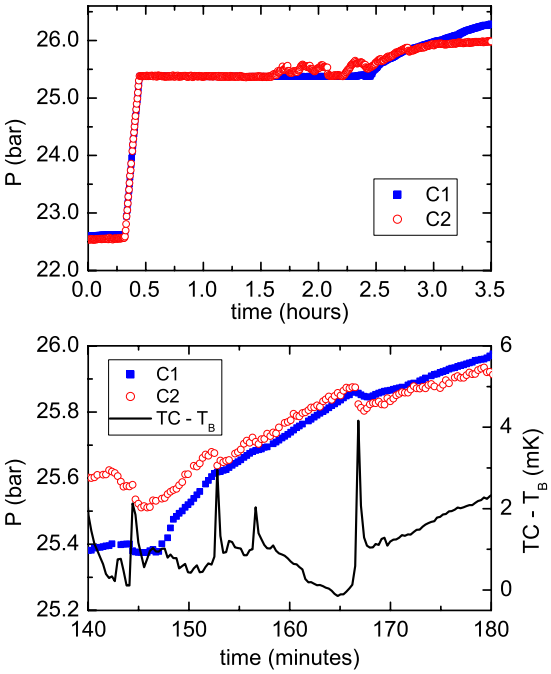

FIG. 5. (Color online) An example of the data from the capacitors C1 and C2 during the growth of a solid sample (sample AB) from the superfluid at fixed temperature. Top: a record of the growth of solid hcp He^4 from the superfluid showing the pressure of the solid in S during growth as measured on capacitors C1 and C2 during an injection of atoms though lines 1 and 2 beginning at $t \approx 0.3$ h. Bottom: An enlarged view of the cell pressure as atoms are fed into S via both V1 and V2. A slowly changing background drift of the cell temperature, TC, was observed and an exponential vs time (T_B) was fit to the data and was pointwise subtracted from TC to enhance visibility of the temperature transients seen on the cell thermometer TC for the cell at TC=415 mK. Transient temperature increases accompany the downward steps in the pressure recorded on C2 and also weakly visible on C1.

tion with the melting curve, P_{melt}, is marked by a sharp change in dP/dT. The trajectory then follows the melting curve until the growth of the solid has finished at which point the cell is filled with bulk solid. While the phase trajectory of the helium in the cell moves down the melting curve, we slowly lower the pressure in fill lines 1 and 2 to closely match the pressure of the cell in a process designed to mimic a fully blocked capillary and limit the migration of atoms into or out of the cell. A modest number of atoms entering the cell through the Vycor should not strongly modify the amount of disorder in the solid which is likely dominated by the substantial pressure and temperature changes encountered as the solid follows the melting curve.

A second approach is to grow the solid from the superfluid at constant temperature. A typical trajectory for this type of growth is shown in Fig. 5 (top figure) for the growth of sample AB (Table I; Appendix A). In this method we add atoms to the cell through capillaries 1 and 2 (which lead to the Vycor). As the pressure in the cell increases it eventually hits the melting curve, and as long as there is still liquid in the cell, the pressure stays constant, and we continue to feed atoms into the cell through lines 1 and 2. Eventually the cell is filled with solid and the pressure can continue to increase. Since those lines do not freeze we can continuously add atoms even after the cell has crossed into the bulk solid region.

An interesting observation, which can be seen in the vicinity of $t=1.5-2.5$ h at the top section of Fig. 5, is the presence of pressure drops that appear in the cell pressure in the vicinity of the melting curve. These pressure drops are accompanied by sharp transient rises in the cell temperature as shown at the lower section of Fig. 5. It is believed that these anomalous events are due to either a reorganization of the crystal or metastable liquid regions freezing, and we have discussed them at greater length separately.[47]

Growing solid helium from the superfluid at constant temperature is thought to produce higher quality crystals as long as the cell pressure $P=P_{\mathrm{melt}}$ since the liquid is superfluid and the pressure is evenly distributed throughout the sample. However, as soon as the pressure rises above the equilibrium melting pressure, the further addition of atoms produces a large amount of stress which most likely results in a highly disordered solid. This is supported by visual observations of solid helium grown this way that document crystals that are cloudy in appearance,[24,48] an indication of a highly disordered solid helium sample.

Another growth technique, which is utilized by the community less frequently, is growth at constant pressure. In this method, the cell is cooled while atoms are continuously fed to the cell through capillaries 1 and 2 to keep the pressure constant. We speculate that because the growth and subsequent cooling will occur at constant pressure, the stresses in the crystal will be smaller, and thus this approach should produce higher quality crystals. None of our experiments to date have utilized this method.

Almost all of the samples grown in torsion oscillators have been grown with the blocked capillary method. Bonfait *et al.*,[22] and Sasaki *et al.*[23] grew crystals from the superfluid; however, they were limited to performing their measurements on the melting curve. It is not yet well understood how crystal growth should effect the behavior recently seen in solid helium. Given the spread in NCRI values reported in the various torsional oscillator experiments, even in ones with cells of similar geometry, it is clear that differences among samples result in substantial differences in the quantitative results.

IV. RESULTS

A. Liquid flow through Vycor

In order to determine the properties of the flow through the Vycor regions contained in V1 and V2, we typically fill region S with liquid helium and measure the flow rate under varying conditions similar to those that we expect to encounter with solid helium in S. Figure 6 shows the results of one of these studies. In this case T1=1.76 K, T2=1.77 K, and TC=412 mK, temperatures that are similar to those present when there is solid in S. There is an offset between the cell pressure and the fill-line pressure which can be accounted for by the fountain effect. The presence of this fountain effect with liquid helium in the apparatus, consistent with expectations, suggests that any parallel liquid flow paths in or

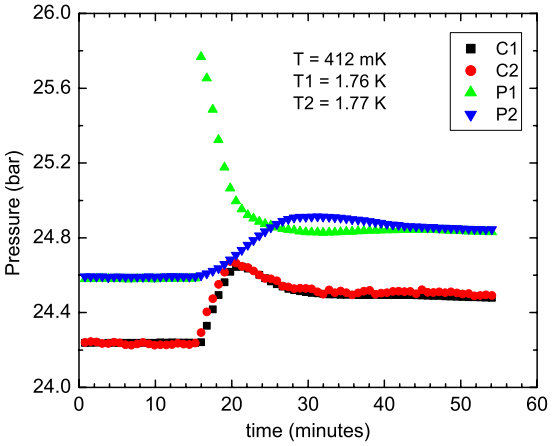

FIG. 6. (Color online) An injection of atoms into line 1 with liquid helium in S began at $t \approx 16$ min. Here T1 and T2 are the temperatures at the liquid reservoirs at the top end of the Vycor rods and TC is the temperature of the cell. P1 and P2 are the pressures at room temperature in fill lines 1 and 2, and C1 and C2 are the capacitive pressure readings at either end of the sample cell. Here, in the region where the rate of change in P2 is linear, $dP2/dt \approx 1.67$ mbar/s. The difference between the pressure read on the capacitors, C1 and C2, and those read on the gauges P1 and P2, ≈ 0.4 bar can be accounted for by the fountain effect.

around the Vycor are rather minor. At $t=16$ min after the data record started, helium was injected into line 1 to create a pressure difference between the two lines. As seen, there is a subsequent increase in the cell pressure and line 2 pressure as atoms flow through the Vycor with equilibrium being achieved at about $t=30$ min. For a span of time P2 changes linearly with time, which should be expected for superflow at a critical velocity. Figure 7 shows the time rate of change in the pressure, $dP2/dt$, in the regime where the pressure changes linearly for various reservoir temperatures, T1 $\approx$T2. As expected the rate decreases as the temperature increases because more normal fluid is in the Vycor at higher temperatures. Note that the upper regions of the Vycor near the reservoirs are outside the superfliud region of the phase

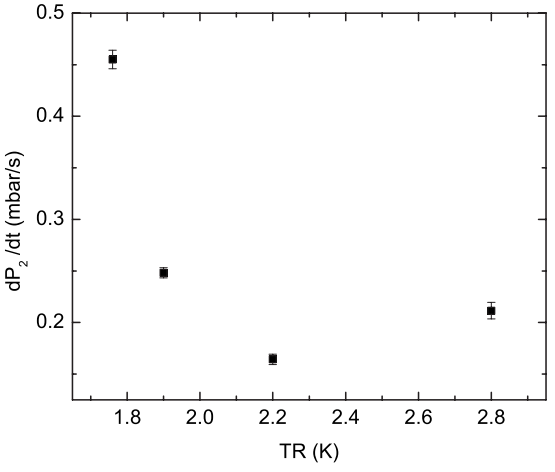

FIG. 7. Rate of pressure change measured in line 2 following an increase in the pressure in line 1 for various reservoir temperatures, TR=T1 $\approx$T2, for cell pressures in the range 23.4 to 23.8 bar.

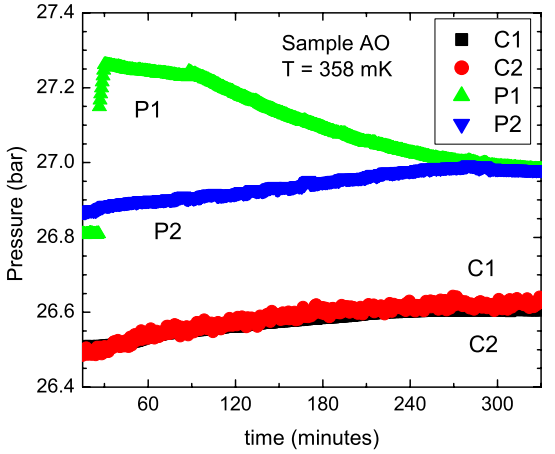

FIG. 8. (Color online) Sample AO, created from superfluid at 358 mK, showed a flow of mass through solid helium. The pressure in R1, P1 was increased at $t \approx 30$ min, the regulator feeding helium to line 1 was closed at $t \approx 90$ min, and changes in pressure were observed for about 5 h. Note that $dP2/dT$ was nearly linear for a substantial duration and independent of P1-P2. Note C1=C2. (For additional comments on C1 and C2, see Sec.V A: discussion of flow and pressure gradients.)

diagram for helium in Vycor. Therefore, some pressure dependence of the flow through the Vycor was anticipated.

Our observed flows through solid helium are a small fraction of the observed limiting flows though Vycor with liquid in the cell. Since our liquid-only flow measurements (of the sort shown in Fig. 6) may be influenced by possible parallel flow channels, we are unable to conclude conclusively that the flows we observe with solid in the cell are unaffected by the flux though the Vycor. While we believe that such effects due to the Vycor are not large (and will comment on this quantitatively later) we recognize that caution is necessary in a discussion of flow-rate limits.

B. Solid helium

After creating a solid in region S, we attempt to document flow through the solid. To illustrate the behavior we will show several examples. The first example is that for a sample (AO: Appendix A, Table I) grown from the superfluid and studied at 358 mK (Fig. 8). After growth, the sample sat idle for ≈ 18 h. For our first measurement on this sample (we call such first-measurement samples "freshly made samples") the detailed data record is started and at $t=30$ min the pressure to line 1 is increased by 0.45 bar and the regulator that feeds atoms into line 1 is closed at $t=90$ min, which terminates the feed. Note that P2 shows a nearly linear increase with time, and the rate of change in P2 with time is independent of P1-P2. This is a very typical example of data that we interpret as evidence for the flow of atoms through the cell filled with solid helium, in this case from line 1 to line 2. The only way for P2 to have increased was for atoms to have moved from R1 to R2 by travel through the solid helium in region S. Hence we can conclude from Fig. 8 that mass has flowed through the cell filled with bulk solid helium. Note

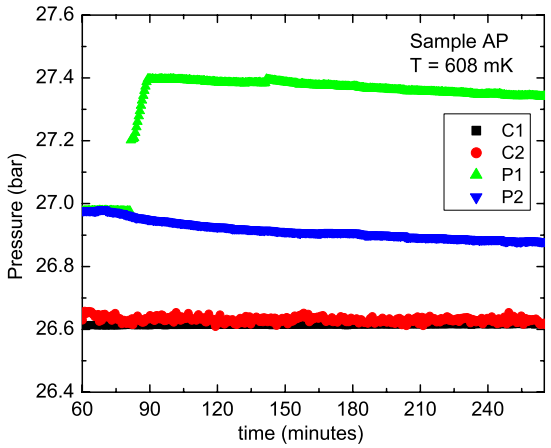

FIG. 9. (Color online) Sample AP, created from sample AO by warming to 608 mK, showed no significant flow of mass through the solid helium. Note C1=C2≈constant.

that the capacitors each record a change in pressure of the solid in the cell.

Following this measurement, the sample was warmed to 608 mK and designated sample AP. (Since this was the second measurement on sample AO, we renamed sample AP and do not refer to AP as a fresh sample.) An attempt to observe flow was then made by application of an increase in pressure to line 1 by 0.42 bar. We interpret the result (Fig. 9) as evidence for no flow. We have observed this behavior on a number of occasions, including one case where P1−P2 =constant≈0.5 bar for nearly 20 h.

Figure 10 shows another data set that provides an example of evidence for flow through a sample of solid helium (sample BS) that was grown from the superfluid. At $t \approx 6$ min P1 was abruptly increased by about 0.4 bar, and atoms were continuously fed into the reservoir via line 1. After $t \approx 30$ min the regulator was shut off and the system was allowed to evolve. We observed an equilibration in P1

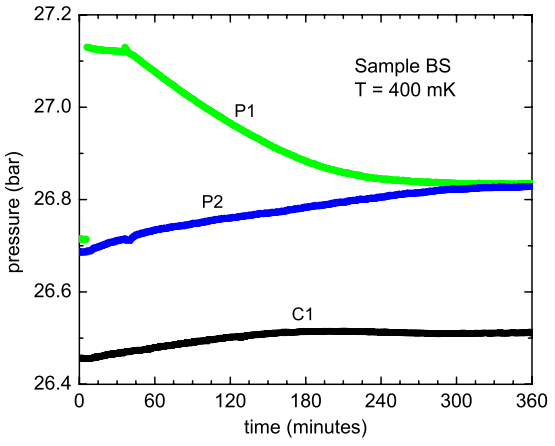

FIG. 10. (Color online) Sample BS showing a flow of mass through solid Helium. The pressure in R1 and P1, was increased at $t \approx 6$ min, the regulator feeding helium to line 1 was closed at $t \approx 30$ min, and changes in pressure were observed for about 6 h. Note that $dP2/dT$ was nearly linear for a substantial duration and independent of P1-P2.

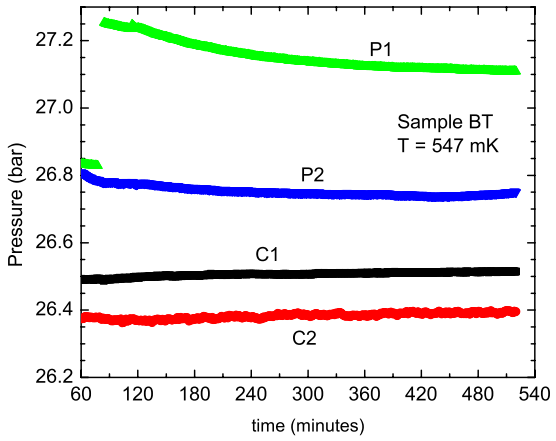

FIG. 11. (Color online) Sample BT was warmed from 400 to 547 mK from sample BS. This is an example of a sample that did not show flow. In this case the regulator fed atoms into R1 for about 30 min, but over 7 h there was no significant movement of the pressures toward equilibrium. Note C1≠C2. (see Sec. V A)

and P2 after about 5 h, an increase in the pressure in S recorded by C1 (measurements from C2 were not available at the time this data set was taken), and a nearly linear increase in P2 while P1 fell.

Although the flow rates observed depend on temperature and pressure, the behavior seen in Figs. 8 and 10 is typical of all cases where we have seen flow. It is interesting to note that in both cases C1, the pressure in S, increased, indicating that *some* of the atoms made their way into the solid but did not move up V2 to the other capillary. This sequence of events is seen every time flow is observed through a sample. That is, upon injection of atoms into line 1, the pressure in the cell and the pressure in line 2 go up in similar fashion to Figs. 8 and 10. One might be led to conclude from the changes in C1 and C2 that plastic flow[49] might be present in the solid helium. We doubt that this is the case because, as we will describe below, we see no such changes in C1 or C2 for cases of similar cell pressure, but higher temperature, where we see no evidence for flow.

Figure 11 presents another example of a sample (BT, which was warmed from BS) that did not show evidence for flow. In this case, P1 was increased by ≈0.422 bar, and atoms were fed in for 30 min. Although P1 did fall for a few hours, after more than 7 h there was no significant movement in the pressures toward equilibrium. Thus we can conclude that no flow was present through this sample.

A significant common difference that is seen between samples that showed flow and those that did not is that in the latter no change in the pressure recorded on C1 and C2 is measured. A number of measurements similar to samples AO/AP and BS/BT have been made. The measurements, sample histories, conditions under which the measurements were made, and flow rates for all of the samples that we have studied are summarized in Table I in Appendix B.

Samples can, of course, be created at higher temperatures. Figure 12 is an example of a sample created at 600 mK. We interpret the results of the application of a pressure increase to line 1 of 500 mbar as evidence for no flow. Another example is shown in Fig. 13 where a sample created at 800 mK

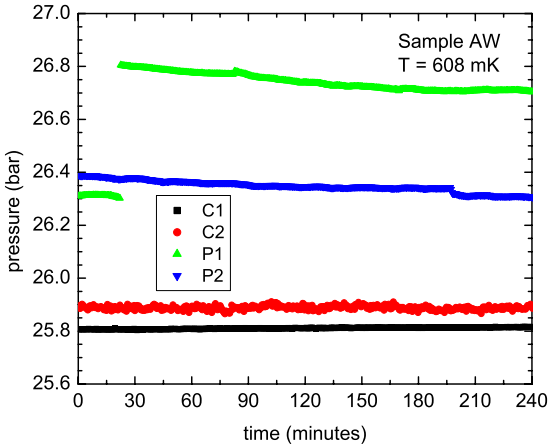

FIG. 12. (Color online) Sample AW, which was created fresh at 608 mK. We interpret this as an example that did not show long term evidence for flow.

showed no evidence for flow. This behavior is typical for all samples we have created at or above 550 mK (or warmed to 550 mK or above); none showed evidence for flow following, at times, initial slow transient behavior.

In Fig. 14 we show the phase diagram coordinates for most of our samples that were freshly made and the results of efforts to observe flow. The data fall into two rather clear regions: samples made at a lower pressure and temperature show flow while those made at higher temperatures or pressures do not.

C. Thermal cycles

Several of the samples listed in Appendix B, Table I, are part of three-step sequences (call the steps a, b, and c) in which, after growing the solid helium, we then added atoms to line 1 and measured $dP2_a/dt$ at a cell Pressure of P_a and temperature T_a. The temperature was then changed to some new value, T_b with pressure P_b (usually higher due to the first addition at T_a), for another addition to line 1, and $dP2_b/dt$ was measured at this new temperature. Finally, we

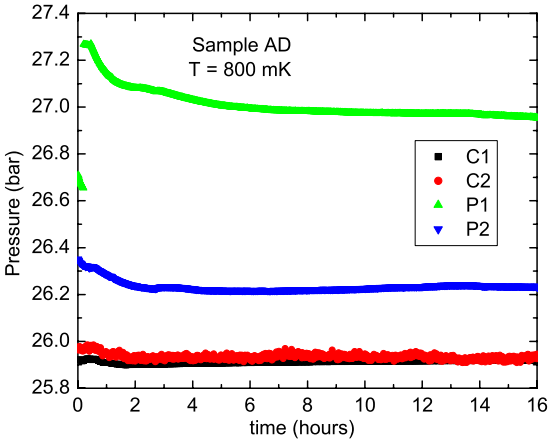

FIG. 13. (Color online) Sample AD, which was created fresh at 800 mK; an example of a sample that did not show evidence for long term flow.

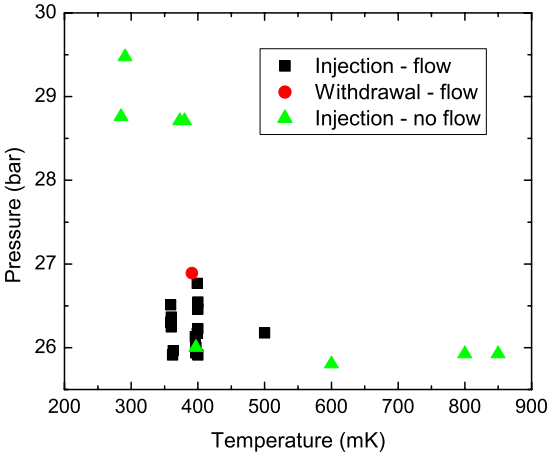

FIG. 14. (Color online) Summary of the results of flow attempts on freshly made samples listed in Appendix B, Table I. For fresh samples, the data fall into rather clear regions of the phase diagram that show flow or no flow. The technique to create a particular sample is tabulated in Table I. The highest pressure samples were grown by the blocked capillary technique.

lowered the sample temperature to T_c which is approximately the original temperature and with pressure, P_c which again was usually a bit higher. A third addition to line 1 produced the measured $dP2_c/dt$.

We have done several of these sequences where we cycle the temperature as described above, and the results are shown in Appendix B, Table II. The previously discussed freshly grown sample, BS, was part of one such sequence (BS-BT-BU). Figure 15 shows the result of the third step, step c, in that sequence; BT was cooled back to the temperature of BS, renamed BU, and the flow rate, which had disappeared for sample BT, returned to nearly the value that was present for sample BS. The flow rate thus appears to have a temperature dependence.

In another example of a temperature cycle sequence (series 3 in Table II), we grew a sample at T=498 mK (P

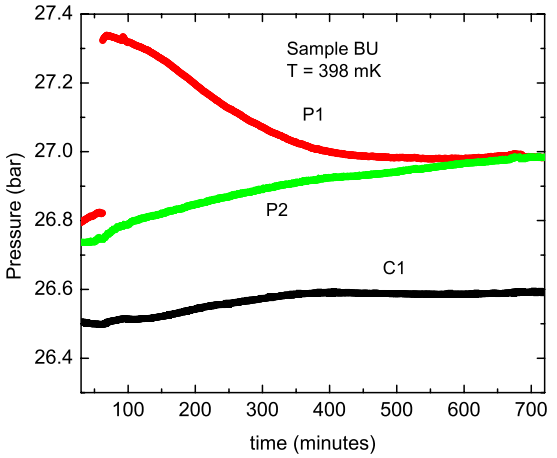

FIG. 15. (Color online) Sample BU, which was cooled from to 547 mK from sample BT and returned to a temperature similar to that of sample BS. The flow seen in sample BU was similar to that seen in sample BS. The measurements made with C2 were not well behaved for this data set and are not shown.

=26.37 bar), then increased P1 by an addition of atoms and observed flow into line 2 (sample AK). The sample was then cooled to 360 mK (sample AL), and P1 increased with flow again observed into line 2; this time at a slightly faster rate then the first time. Finally the sample was warmed back to 498 mK (sample AM) and at a still higher pressure of 26.71 bar. A final injection of atoms to this sample produced a behavior that was reminiscent of both flow and no flow; the pressure, P1, decreased after shutting off the regulator while C1 and C2 both increased; however, the pressure in line 2 did not rise, implying that there was actually no helium flow through V2.

This sequence was then repeated with a new sample, which was grown cold then warmed (series 6, BD, $T=390$ mK, and $P=25.86$ bar). In this case, flow was observed at 400 mK, but not at 500 mK, though at 500 mK, again, C1 and C2 increased with P1 decreasing. When the sample was cooled back to 400 mK, the addition of helium to line 1 produced no flow into line 2 for 60 min after which a rather fast flow was observed.

The observations on the behavior of the flow for a sample warmed to 500 mK, coupled with the absence of flow at 550 mK and above, lead us to believe that at the pressure at which the sample was studied perhaps there is a transition between a flow state and a nonflow state around $T=500$ mK. We thus did two more thermal cycles this time, warming the sample to 450 mK. The first, series 7 (Samples BJ, BK, and BL), showed the same behavior as the 500 mK samples with P1 decreasing, C2 and C1 increasing, and P2 staying constant and then again the same behavior when cooled back to 400 mK. The second cycle (series 8, samples BP, BQ, and BR), however, showed a clear flow and relaxation at 450 mK and then again when cooled back to 400 mK. As previously described, the final sequence, series 9, BS-BT-BU, was warmed to 547 mK and showed no flow; then when cooled back to 400 mK, the flow returned. Measured near the untimely end of our data run, this is the only clear example to date for which we have seen a return to a nearly equal flow rate, following the observation of no flow at higher temperatures, without first performing a withdrawal.

V. DISCUSSION

A. Flow and pressure gradients

Several conclusions can be immediately drawn from the data shown in Table I. First, the method of solid growth seems to have no effect on whether or not flow is observed. Several samples grown from the superfluid have shown flow (for instance sample A) and several have not (sample H). Likewise we have observed flow in some samples grown by the blocked capillary method (sample V), and we have also made samples by the blocked capillary method that have not shown flow (sample D). We find it curious, however, that samples created by the blocked capillary technique and cooled at approximately constant pressure once off the melting curve can show flow, while samples created from the superfluid at or warmed to 800 mK do not show flow when subsequently cooled. Differences in cooling rates or defects in the various samples may be involved.

While most of the runs listed in Table I were done by injecting atoms into reservoir 1, one of them (sample U) was an injection into reservoir 2, and it showed flow. Additionally, we have several times attempted a subtraction of pressure in reservoir 1 (a procedure we have termed as a "pull" or a "withdrawal"). In each instance a withdrawal produced a flow of atoms from the opposite reservoir (i.e., a "withdrawal" from reservoir 1 produced a corresponding drop in pressure in reservoir 2). It is possible to induce a flow of mass in either direction.

As mentioned previously, the flow rates seen in Figs. 8 and 10 are constant in time and independent of the pressure difference between the two fill lines; $dP2/dt \approx$ constant. This is reminiscent of a superflow flowing at a limiting velocity, where the flow rate should be independent of the pressure head. Here it is useful to return to the possible influence of the Vycor on the measured flow rates through the solid helium. If the Vycor were indeed causing an upper limit to the flow (as opposed to the solid itself), then fresh samples grown at the same temperature and pressure should show the same flow rate. We have a few fresh samples that were grown at the same temperature and pressure. Samples AB and BO are one example of such a pair; both were fresh at 26 bar and 398 mK. For sample AB, $dP/dt=0.0230$ mbar/s, a much faster flow than BO for which $dP/dt=0.0095$ mbar/s, each had a similar pressure step. Another example is present in samples AN and AR, which were both grown at 359 mK. AN was at a pressure of 26.30 bar and had a flow of 0.0203 mbar/s. AR was at 26.25 bar, nearly the same pressure, with a flow rate of 0.0088 mbar/s. Both had similar Vycor temperatures and similar pressure steps. Certainly the flux through the Vycor did not limit the lower flow rates observed for the two sample pairs. Examples such as this provide evidence that we are indeed observing critical flow limitation in the solid, limitation that is sample dependent and not Vycor dependent. It would be useful to repeat observations of this sort under the same conditions with varying initial pressure increases to see if that affects the flow rate. This is difficult to accomplish in practice because the pressure of the cell changes with each injection, and separately prepared samples may have different flow properties (due to different configurations or different numbers of flow paths).

We find that the pressures recorded by C1 and C2 on opposites ends of the cell are often different. $\delta C=C1-C2$ can sometimes differ by several tenths of a bar and remain stable (independent of the presence or absence of a flow), which means that the solid lattice can support and maintain a pressure gradient across the solid (which provides further evidence against the presence of plastic flow). These pressure gradients tend to occur after the solid is off the melting curve but while we are still adding atoms to it during the growth process. Sometimes we see a relaxation of the pressure during a measurement, but oftentimes these pressure gradients persist until the solid is melted. The presence of pressure gradients sustained in the solid seems to have no effect on the flow. We have seen flow occur when $C1=C2$, i.e., $\delta C=0$ (e.g., Fig. 8) and also when $C1 \neq C2$, i.e., δC

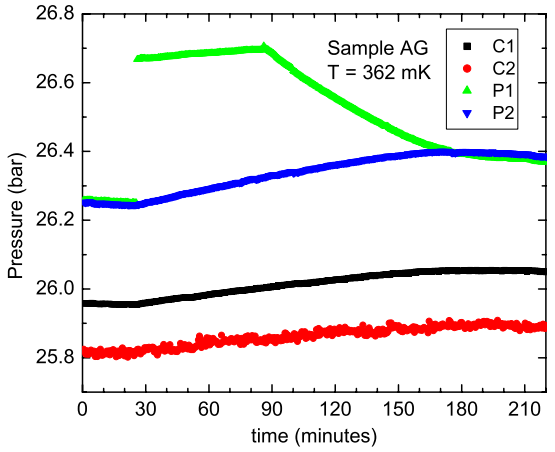

FIG. 16. (Color online) Sample AG, created from superfluid and studied at 362 mK, showed a flow of mass through solid helium. Note in this case that C1 and C2 were not equal; (compare to Fig. 8).

$\neq 0$ (e.g., Fig. 16), which implies that the flow is not directly related to pressure gradients within the solid. As stated previously, when no flow is observed we also observe no change in C1 and C2, with C1=C2 (e.g., Fig. 9) or with C1 $\neq$ C2 (e.g., Fig. 11). We believe the reason for this is that in order for C1 and C2 to record a pressure change, mass must move from the liquid in the Vycor to the pressure gauges located on the ends of the solid. Whatever mechanism is transporting the mass from V1 to V2 is likely also responsible for moving the mass to the ends of the solid. With the conducting paths no longer able to support mass flow, there is no way to move mass to the ends of the cell where the pressure gauges are since we know from Day and Beamish[20] and Day *et al.*[19] that squeezing the lattice cannot produce any mass flow. It should therefore come as no surprise that we see no pressure change in the solid when no flow is observed. These observations further appear to make unlikely plastic flow[49] as a flow mechanism since it should occur even if any conducting paths in the solid are unable to conduct mass.

B. Possible hysteresis

The data we have collected to date point to a temperature dependence with possible hysteretic behavior. All of the samples created from superfluid at, or cycled to, $T \geq 550$ mK showed no flow, even if they showed flow at lower temperatures, and further, no flow is typically observed after cooling a sample from $T \geq 550$ mK, i.e., a sample that was previously grown at or warmed to $T \geq 550$ mK from a lower temperature. These thermally cycled samples, however, could be made to flow again by applying a withdrawal, and subsequent injections after such a withdrawal produced flow through the sample. But, we have also performed a withdrawal on a sample created and measured at 600 mK which showed no evidence of flow. This is important because samples at lower temperatures almost always flowed during a withdrawal. We can thus conclude that solid helium created from superfluid at, or warmed to $T \geq 600$ mK does not support flow. Furthermore, samples warmed to and then cooled from $T \geq 600$ mK also do not flow without first withdrawing atoms from one fill line. On the other hand, samples warmed to 500 mK tend to show some elements of flow, but mass does not flow into line 2. It appears as if at these temperatures the flow paths are on the edge of a transition from a flow state to a no flow state (or absence of continuity of the conducting path across the sample). The data thus point to a scenario wherein whatever conducts the flow ceases to do so for $T \geq 550$ mK.

Our data have also led us to believe that the liquid channels responsible for the results of Sasaki *et al.*[24] are likely *not* responsible for the flow observed in our samples. Liquid channels, as described by Sasaki *et al.*,[24] should be superfluid at temperatures well above 1 K, which is contrary to what we have observed. All samples warmed to or created at temperatures >550 mK show no flow by either "injection" or "withdrawal," meaning that flow ceases in whatever is conducting the mass flow through the solid (or the conducting pathway disappears) at these temperatures. Annealing is unlikely since we are well outside the temperature range where annealing takes place on the time scales of our measurements, and we see none of the effects of annealing that other laboratories see, such as a decrease in the pressure of the sample[15,46] that is seen when samples are close the melting curve. We think it more likely that we are seeing flow along structures, such as dislocations and grain boundaries imbedded in the solid, which are predicted to be superfluid.[30,31] In fact, Pollet *et al.*[30] predicted that grain boundaries should become superfluid for $T \sim 500$ mK, a prediction perhaps supported by our data that show flow that stops at and above 550 mK. In almost all cases when we have warmed samples to temperatures above 550 mK, we do not see flow when the sample is cooled. This could point to a hysteresis in the flow behavior (i.e., flow might once again appear if we were able to get the sample colder). Although we cannot yet unambiguously rule out mass flow along liquid channels as an explanation for our observations, we feel that the data point more strongly to flow along defects, although the matter is far from completely settled.[50,51]

C. Quantitative aspects

The data from Fig. 10 (sample BS) and other data like them can be used to characterize the flow and to make quantitative comments relevant to what may be causing the flow. The mass flux of a superfluid with density ρ through a conduit of cross section A and velocity v can be written as

$$\frac{dm}{dt} = \rho v A. \tag{1}$$

For sample BS, using the time that we fed atoms into line 1, 30 min, and the rate at which the pressure in P1 falls immediately after ceasing the addition of atoms, we can estimate that we supplied as an upper limit an amount of mass $\Delta m_1 \approx 1.1 \times 10^{-4}$ g. Of this mass, $\approx 6.6 \times 10^{-5}$ g joined the solid, while $\approx 4.6 \times 10^{-5}$ g flowed through the solid and into line 2. Thus, the average rate that mass flowed into line 2 can be estimated as $dm_2/dt \approx 2.2 \times 10^{-9}$ g/s. Ignoring possible effects due to the Vycor, if this flow is along dislocations

pervasive throughout the solid as predicted by Boninsegni *et al.*,[31] then we can take as our conducting pathways tubes with a diameter of atomic dimensions, 0.5 nm. If we assume that the critical velocity is on the order of that in a thin helium film, then we can take $v \sim 200$ cm/s. Putting these numbers into Eq. (1) and using $\rho \approx 0.19$ g/cm^3 as the density give a mass flow through one dislocation of $\approx 7.5 \times 10^{-14}$ g/s, and thus it would take something on the order of 2.9×10^4 dislocations to account for the mass flow we observe in Fig. 10. We can compute similar numbers for the other measurements from Table I. If we take measurements done on freshly prepared samples at $T = 400 \pm 4$ mK and $P = 26.1 \pm 0.2$ bar we see the number of dislocations needed to support the flow range in number from $\approx 2 \times 10^4$ to $\approx 5 \times 10^4$. Using the cross-section area of S between the Vycor rods, 0.3 cm^2, we can compute the dislocation density for these samples to be in the range of $6-16 \times 10^4$ cm^{-2}.

We can do a similar analysis assuming that the conducting defects are grain boundaries instead of dislocations. If our solid sample contains one grain boundary that spans the entire diameter of the cell and is one atomic layer thick, then the cross sectional area of the conducting path is $A = 3.2 \times 10^{-8}$ cm^2. Then, using Eq. (1) and taking account of the fact that the intersection with the Vycor is a length less than the diameter of the cell, we can compute the velocity of the mass flowing through this pathway as $v \approx 1$ cm/s. Instead, if we were to take the velocity of flow along the gain boundary to be 200 cm/sec, then a grain boundary of atomic thickness would need be only 0.001 cm in width; i.e., the grain boundary only spans a portion of the cell, which seems unrealistic.

We must also explore quantitatively the possibility of liquid channels proposed by Sasaki *et al.*,[24,25] which were discussed earlier. They suggest that the size of the liquid channels depends on $1/\Delta P_{\rm eq}^2$, where $\Delta P_{\rm eq}$ is the difference between the solid pressure and the solid-liquid equilibrium pressure. If we adopt the view that liquid channels are indeed present, then following Sasaki *et al.*[24,25] we can write the cross sectional area of the channel, $A_{\rm LC}$, as

$$A_{\rm LC} = R^2 \left[2\sqrt{3} \sin(\phi) \sin\left(\phi + \frac{\pi}{3} \right) - 3\phi \right]. \tag{2}$$

Here $\phi = \pi/6 - \theta$, where $\theta \approx \pi/12$ is the contact angle between the grain boundaries and R is the radius of curvature between the liquid and solid phases, which is given by

$$R = \frac{\rho_S}{\rho_S - \rho_L} \frac{\sigma_{\rm LS}}{\Delta P_{\rm eq}}, \tag{3}$$

where $\rho_S = 0.19$ g/cm^3 and $\rho_L = 0.17$ g/cm^3 are the solid and liquid densities and $\sigma_{\rm LS} = 1.7 \times 10^{-4}$ N/m is the liquid-solid surface tension.

To show the observed effect of cell pressure in our experiments, we have plotted in Fig. 17 the mass flow rate into capillary 2 as a function of starting sample pressure for all of our freshly made samples created at a temperature of $T \approx 400$ mK. Although it is difficult to make comparisons about flow rates of separately prepared solid samples since the number of conducting pathways or configurations can be different for each sample, it is clear that there is a general

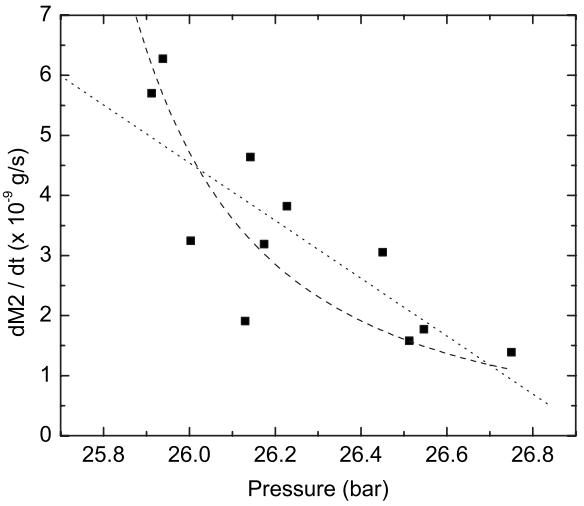

FIG. 17. Rate of change in mass in reservoir 2 after injecting atoms into reservoir 1 as a function of initial sample pressure. All samples portrayed here were freshly grown in the vicinity of 400 mK. The curved line is a fit to the data under the assumption that liquid channels carry the flow [Eq. (2)]. The straight line is an arbitrary straight-line fit. The quality of the fit is nearly the same in each case.

trend of decreasing flow rate for increasing sample pressure. Figure 17 suggests that at $T \approx 400$ mK there might be a sample cell pressure above which the mass flux is $\approx$ zero. It is possible that there is a temperature-dependent critical pressure, $P_H(T)$, such that at temperature T no flow is observed above that pressure. If this is the case then it means that for TC ≈ 550 mK, $P_H \approx P_{\rm melt}$.

Equation (1) with Eq. (2) as the cross-sectional area of the flow path is also plotted in Fig. 17 as the curved line with a limiting velocity taken[52] to be 800 cm/s and the number, N, of liquid channels used as a fitting parameter. The fit results in $N = 57$ liquid channels spanning the distance between the Vycor Rods, which should be interpreted as an average number for the set of samples included. The fit is reasonable, but there is much scatter in the data, and a linear fit (also shown) works equally well. We take the result as suggestive, but our observations that no flow is ever observed at temperatures greater than 550 mK remain unexplained by the liquid channel scenario. As we have pointed out,[51] presuming such channels remain present, they should continue to conduct above 550 mK and be present for samples made fresh at and above this temperature. But, we have not been able to observe flows for $T \geq 550$ mK. Thus, we believe that the weight of the evidence does not favor liquid channels as the source for our observations.

Finally, we might assume that the mass is conducted not along defects but through the actual solid such as in a superglass phase that has been predicted to occur in highly disordered samples.[32,34,35] In this case, we can modify Eq. (1) slightly to include a dimensionless term ξ which represents the fraction of the solid that is in flux (if this were a superfluid, ξ would denote the superfluid fraction) so that

$$\frac{dm}{dt} = \xi \rho v A. \tag{4}$$

In this case A is the cross-sectional area of S between the Vycor rods. (An alternate perspective is to assume that A is the open cross sectional area of the pores in the Vycor, where they meet the solid. Below, numbers in parentheses are based on this alternate perspective.) For the data in Fig. 10 we find that $v\xi = 2.9 \times 10^{-9}$ cm/s ($v\xi = 1.2 \times 10^{-8}$ cm/s). If we take $\xi \approx 0.01$ (as is typical of a number of the NCRI measurements), then $v \approx 2.9 \times 10^{-7}$ cm/s ($v \approx 1.2 \times 10^{-6}$ cm/s). If instead we arbitrarily take $v = 100$ μ/s, then $\xi = 2.9 \times 10^{-6}$ ($\xi = 1.2 \times 10^{-5}$). For the freshly made samples at 400 mK and 26.1 bar, with $v = 100$ μ/s, we find ξ to be between 3×10^{-6} and 8×10^{-6} (1.2×10^{-5} and 3.2×10^{-5}). These numbers are, of course, highly dependent on the arbitrary estimate we used for the critical velocity, but we can note that ξ is several orders of magnitude less than the superfluid fraction reported by Kim and Chan[10] in their bulk solid measurements of NCRI.

D. Chemical potential

Since, as we have stated before, we are inducing flow by creating a chemical-potential difference across the solid, it is perhaps useful to use the pressure and temperature data to calculate the chemical-potential difference applied across the solid. The chemical potential, μ, can be found from

$$\mu(P,T) = \int \frac{V}{N} dP - \int \frac{S}{N} dT, \tag{5}$$

where V is the volume, S is the entropy, and N the number of atoms. Using $N = \rho V / m_4$, where m_4 is the mass of a helium atom, and defining the specific entropy s as the entropy per unit mass, $s = S/\rho V$, Eq. (5) becomes

$$\mu(P,T) = m_4 \left(\int \frac{dP}{\rho} - \int s dT \right). \tag{6}$$

It is sufficient in our case to calculate the chemical potential of only the liquid above the Vycor. In the Vycor there should be no chemical-potential difference since the flow is likely below critical velocity (as we can tell from our measurements of the flow of atoms through our system, e.g., Figure 7). So by computing $\Delta\mu$ bewteen the tops of the Vcyor rods, which are at a temperature of $T \approx 1.8$ K, we can find the chemical-potential difference that is driving the flow through the solid. Using Eq. (6), we compute the chemical potential for each side and then take the difference, $\Delta\mu = \mu_1 - \mu_2$. Figure 18 shows the measured flow rate into line 2 vs the applied chemical-potential difference across the solid at $T = 396 \pm 4$ mK and for pressures of 26.5 ± 0.1 bar and 26.1 ± 0.1 bar. Although there is considerable scatter, it appears that the flow rate into line 2 is independent of the chemical-potential difference between the two lines, which provides further evidence of superflow at critical velocity. It also seems that the flow rate in samples at the higher pressure of 26.5 ± 0.1 bar is lower than the flow rate for the lower pressure samples regardless of the applied $\Delta\mu$. Although, as mentioned before, there is no reason why two separately prepared samples should have the same flow rate given the same parameters (sample pressure, $\Delta\mu$, etc.); Fig. 18 does seem to show that there may be dependence of the flow rate on the sample pressure.

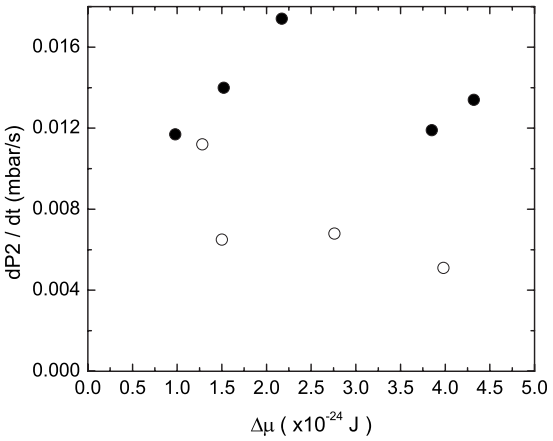

FIG. 18. Flow rate into line 2 versus the applied chemical-potential difference across the solid for fresh samples at $T \approx 400$ mK. Open circles are at $P = 26.5 \pm 0.1$ bar and closed circles are at $P = 26.1 \pm 0.1$ bar.

VI. SUMMARY

We have performed experiments in which a chemical-potential difference is applied across hcp solid ^{4}He at low densities by injecting liquid helium into one side of the solid and have observed a dc mass flow. The flow is observed at temperatures below approximately 550 mK and at pressures below approximately 26.9 bar. The flow rate is mostly constant over time, and it is independent of the applied chemical-potential difference which leads us to believe that we are seeing a superflow at close to critical velocity, mindful of our earlier caution about the possible effects of the Vycor. The flow rate is dependent on the pressure of the solid with flow substantially reduced by 27 bar at 400 mK. It is our thought that this pressure dependence of the flow is itself a function of temperature, and as we move to lower temperatures in future work the maximum pressure at which we see flow may increase; indeed, in more recent work we have seen clear evidence for flow at 120 mK and 28 bar. We have also observed that samples thermally cycled to, or above, 550 mK do not support flow again when cooled down without first subtracting pressure from one of the fill lines. This behavior could suggest hysteresis, and in order to restore flow without a withdrawal of pressure, we may have to get to lower temperatures. This behavior could also be caused by defects introduced into the solid by the process of withdrawal.

We conjecture that, based on the current evidence, the flow is being conducted along defects in the solid, such as has been predicted theoretically for grain boundaries and dislocations. We do not believe that the flow is along the liquid channels shown to exist by Sasaki *et al.* [24] for the primary reason that at 550 mK, the temperature at which we cease to

see flow, these liquid channels should still be superfluid. Even if these liquid channels did cease to conduct flow at such temperatures, presuming that they remain in place, there is then no reason why flow should not return upon cooling the sample again. There also seems to be no reason why they should not be present in fresh samples made for $T \geq 600$ mK.

Finally, the relationship between our experiment and other solid helium experiments, mainly the torsion-oscillator experiments and the shear-modulus experiments, is yet to be determined, and the only way to concretely establish such a relationship will be to extend our results to lower temperatures. It is possible that, as shown by our much lower "superfluid" fraction, we are seeing some precursor effects of the mechanism that is causing the NCRI in the torsion oscillators, which is not visible to them due to the very small effective NCRI fraction implied by our measurements. Indeed, many torsional oscillator experiments begin to see evidence for period shifts in the vicinity of 250–300 mK. With enhanced sensitivity it is possible that they would see evidence for NCRI at higher temperatures. This makes measurements at lower temperature of the utmost importance.

ACKNOWLEDGMENTS

We would like to thank B. Svistunov and N. Prokofev for discussions that motivated this experiment. We also thank S. Balibar and J. Beamish for helpful advice on the growth of solid helium and for many productive conversations. Also, F. Caupin, M. C. W. Chan, R. A. Guyer, E. Kim, H. Kojima, M. W. Meisel, W. J. Mullin, J. D. Reppy, S. Rittner, E. Rudavaskii, and Ye. Vekohov provided many useful comments and discussions. This work was supported by NSF (Contracts No. DMR 06-50092 and No. CDRF 2853) and by access to the facilities provided by the MRSEC at the University of Massachusetts Amherst supported by NSF (Contracts No. DMR 02-13695 and No. DMR 08-20506).

APPENDIX A: UNUSUAL OBSERVATIONS

While most of our data sets that showed clear evidence for flow behaved in a common way (P2 increased linearly with time and the pressures recorded on the cell capacitors increased), and occasionally we saw changes in the cell pressure with more limited changes in P2, we did see one rather unusual data set. A sample was grown fresh as sample BV and flowed at 399 mK. It was then injected again (sample BW) and showed no evidence for flow. It was then subjected to a withdrawal (sample BX) and again showed no evidence for flow, an unusual event for a withdrawal. It was then subjected to further injection (sample BY) and showed evidence for flow that then stopped prior to equilibration (Fig. 19). A subsequent injection (sample BZ) resulted in a normal flow to equilibration (Fig. 20). An additional injection (sample CA) showed typical further evidence for flow. There were few anomalous situations such as described by the sequence BV-CA, and we simply note this one here to be complete.

APPENDIX B: TABLES OF SAMPLE CHARACTERISTICS

Here we list each of the samples of solid helium that we have studied (Table I) and each of the sets of samples for which we have done thermal cycling sequences (Table II). In Table I we list each sample by the code letter that was assigned to it. Samples were created or studied in the order of the code letters in almost all cases. Note that a new code letter was given to a sample each time a change was made in the sample. So, for example, sample A was grown fresh from superfluid, so was sample B, but sample C was the code given to sample B after it had been warmed to 1.25 K. Missing code letters indicate samples that were useless or untrustworthy for one reason or another (e.g., temperature instabilities in the apparatus, a helium transfer midrun, etc.).

Table II is a tabulation of sets of samples that were part of a sequence of measurements that began with the sample with code letter indicated in the first column. So, for example, the first entry represents a sequence that began with sample M, which was created from superfluid at 392 mK. Sample M

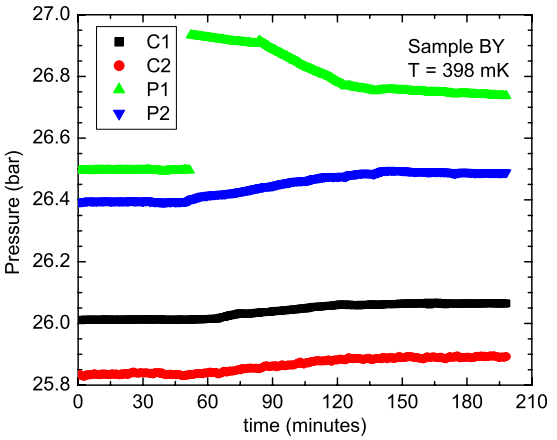

FIG. 19. (Color online) Sample BY, which showed the unusual behavior of a flow that stopped before equilibration.

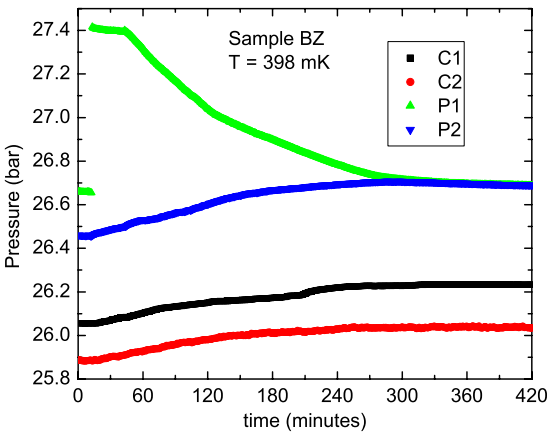

FIG. 20. (Color online) Sample BZ, which showed the more normal behavior of flow to equilibration, P1=P2. Sample BZ, is the same sample as BY, designated BZ with an injection following the completion of the behavior seen in Fig. 19.

TABLE I. Table of flow measurements made for the solid Helium flow experiments showing: (1) sample: each measurement was deemed a separate sample; (2) run: each run was a chain of samples all from the same growth; (3) history: either how the sample was grown or what sample it came from; (4) sample temperature; (5) sample pressure (6) initial pressure step put into line 1; and (7) flow rate observed in line 2. (a) Pressure added to line 2. (b) A first addition of 0.41 bar showed no flow over 6.5 h. (c) Subtraction from line 4. (d) A number of small pressure steps (0.2 bar).

Sample	Run	History	T_{sample} (K)	P_{sample} (bar)	ΔP_i (bar)	$dP2/dt$ (mbar/s)
A	sf1-3a_sh1	Superfluid	0.398	26.75	1.482	0.0051
B	sf1-3a_sh2	Superfluid	0.386	26.41	1.752	0.0290
C	sf1-3a_sh2	B	1.25	25.65	2.432	0.0000
D	sf1-3_sh5	Blocked capillary	0.285	28.76	1.705	0.0000
E	sf1-3_sh5	D	0.900	28.82	1.775	0.0000
F	sf1-3_sh4	Blocked capillary	0.380	28.70	2.156	0.0000
G	sf1-3b_sh1	Superfluid	0.380	26.68	1.779	0.0027
H	sf1-3b_sh1	G	0.444	27.30	0.778	0.0000
J	sf1-3b_sh1	H	0.460	27.24	1.797	0.0000
K	sf1-3b_sh1	J	0.420	27.16	−2.233	−0.0127
L	sf1-4b_sh2	Superfluid	0.391	26.89	−1.221	0.0472
M	sf1-3b_sh2	Superfluid	0.392	26.36	0.950	0.0121
N	sf1-3b_sh2	M	0.804	26.54	1.032	0.0000
O	sf1-3b_sh2	N	0.384	26.52	1.005	0.0000
P	sf1-3b_sh2	O	0.384	26.52	−2.300	−0.0804
Q	sf1-3b_sh2	O	0.400	25.93	0.616	0.0067
R	sf1-3b_sh2	Q	0.396	26.13	0.801	0.0075
S	sf1-3b_sh3	Blocked capillary	0.400	27.25	−2.718 c	−0.0667
T	sf1-3b_sh3	Blocked capillary	0.392	26.51	0.691 a	0.0171
U	sf1-3b_sh4	Blocked capillary	0.380	26.54	0.541 a	0.0120
V	sf1-3b_sh5	Blocked capillary	0.395	26.13	0.844	0.0070
W	sf1-3b_sh6	Blocked capillary	0.290	29.48	0.582	0.0000
X	sf1-3b_sh7	Superfluid	0.393	26.13	1.062 b	0.0134
Y	sf1-3b_sh7	X	0.391	26.43	0.462	0.0093
Z	sf1-3b_sh7	Y	0.818	26.83	0.465	0.0000
AA	sf1-3b_sh7	Z	0.388	26.79	0.457	0.0000
AB	sf1-3b_sh8	Superfluid	0.398	25.95	0.430	0.0230
AC	sf1-3b_sh8	AB	1.02	25.93	0.518	0.0000
AD	sf1-3b_sh9	Superfluid	0.800	25.93	0.483	0.0000
AE	sf1-3b_sh10	Superfluid	0.850	25.93	d	0.0000
AG	sf1-3c_sh1	AF	0.363	25.95	0.414	0.0195
AH	sf1-3c_sh2	Superfluid	0.363	25.92	0.723	0.0434
AJ	sf1-3c_sh4	Superfluid	0.498	26.18	0.633	0.0111
AK	sf1-3c_sh4	AJ	0.498	26.37	0.443	0.0026
AL	sf1-3c_sh4	AK	0.359	26.52	0.818	0.0076
AM	sf1-3c_sh4	AL	0.498	26.69	0.423	0.0000
AN	sf1-3c_sh5	Superfluid	0.359	26.30	0.473	0.0203
AO	sf1-3c_sh6	Superfluid	0.358	26.51	0.451	0.0076
AP	sf1-3c_sh6	AO	0.608	26.61	0.421	0.0000
AQ	sf1-3c_sh6	AP	0.358	26.62	0.350	0.0000
AR	sf1-3c_sh7	Superfluid	0.359	26.25	0.391	0.0088
AS	sf1-3c_sh7	AR	0.608	26.37	0.531	0.0000
AT	sf1-3c_sh7	AS	0.359	26.36	0.548	0.0000
AU	sf1-3c_sh7	AT	0.359	26.37	−1.307	−0.0302

TABLE I. (*Continued.*)

Sample	Run	History	T_{sample} (K)	P_{sample} (bar)	ΔP_i (bar)	$dP2/dt$ (mbar/s)
AV	sf1-3c_sh7	AU	0.358	26.39	0.662	0.0054
AW	sf1-3c_sh8	Superfluid	0.608	25.81	0.500	0.0000
AX	sf1-3c_sh8	AW	0.600	25.82	−0.793	0.0000
AY	sf1-3c_sh8	AX	0.360	25.78	0.489	0.0000
BA	sf1-3c_sh9	Superfluid	0.360	26.37	0.538	0.0043
BC	sf1-4_sh1	Superfluid	0.400	25.91	0.606	0.0209
BD	sf1-4_sh1	BC	0.390	25.86	0.664	0.0146
BE	sf1-4_sh1	BD	0.498	26.03	0.542	0.0000
BF	sf1-4_sh1	BE	0.394	26.10	0.394	0.0364
BJ	sf1-4_sh3	Superfluid	0.397	26.45	0.449	0.0112
BK	sf1-4_sh3	BJ	0.452	26.52	0.432	0.0000
BL	sf1-4_sh3	BK	0.397	26.58	0.398	0.0000
BM	sf1-4_sh3	BL	0.396	26.50	0.277	0.0000
BO	sf1-4_sh4	Superfluid	0.398	26.03	0.427	0.0095
BP	sf1-4_sh5	Superfluid	0.400	26.23	0.418	0.0140
BQ	sf1-4_sh5	BP	0.449	26.53	0.475	0.0058
BR	sf1-4_sh5	BQ	0.400	26.52	0.416	0.0039
BS	sf1-4_sh6	Superfluid	0.400	26.45	0.414	0.0065
BT	sf1-4_sh6	BS	0.547	26.49	0.419	0.0000
BU	sf1-4_sh6	BT	0.398	26.50	0.515	0.0052
BV	sf1-4_sh7	Superfluid	0.399	26.17	0.558	0.0117
BW	sf1-4_sh7	BV	0.398	26.18	0.918	0.0000
BX	sf1-4_sh7	BW	0.398	26.18	−1.122	0.0000
BY	sf1-4_sh7	BX	0.398	26.01	0.437	0.0178
BZ	sf1-4_sh7	BY	0.398	26.06	0.748	0.0215
CA	sf1-4_sh7	BZ	0.397	26.23	0.573	0.0145

was then warmed to 804 mK (and denoted sample N, Table I). Following measurement at 804 mK, sample N was cooled to 384, renamed sample O, and studied. Table I shows such triples. Note also that for some of these sequences of three, such as M, N, and O, a continuation of the sequences (e.g., P, Q, and R) took place, which can be seen in Table I.

TABLE II. Thermal cycling of solid helium samples and its effect on flow through the sample. A given series begins the sample denoted in parentheses in column 1. Temperatures and pressures are those of the cell. In all cases atoms were added to line 1 and $dP2/dt$ is the measured rate of change in P2. (a) No change in the pressure of P2 was recorded for 60 min followed by rapid pressure relaxation. (b) No change in P2 was recorded; however, the cell pressure increased and P1 decreased.

Series	T_A (mK)	P_A (bar)	$dP2_A/dt$ (mbar/s)	T_B (mK)	P_B (bar)	$dP2_B/dt$ (mbar/s)	T_C (mK)	P_C (bar)	$dP2_C/dt$ (mbar/s)
1 (M)	392	26.36	0.0121	805	26.54	0.0000	385	26.52	0.0000
2 (Y)	391	26.43	0.0093	818	26.83	0.0000	388	26.79	0.0000
3 (AK)	498	26.37	0.0026	360	26.52	0.0076	498	26.69	0.0000b
4 (AO)	358	26.51	0.0076	608	26.61	0.0000	358	26.62	0.0000
5 (AR)	359	26.25	0.0088	608	26.37	0.0000	359	26.36	0.0000
6 (BD)	390	25.86	0.0146	498	26.03	0.0000b	394	26.10	0.0364a
7 (BJ)	397	26.45	0.0112	452	26.52	0.0000b	397	26.58	0.0000b
8 (BP)	400	26.23	0.0140	449	26.53	0.0058	400	25.52	0.0039
9 (BS)	400	26.45	0.0065	547	26.49	0.0000	398	26.50	0.0052

[1] W. J. Mullin, Phys. Rev. Lett. **26**, 611 (1971).
[2] H. Matsuda and T. T. Tsuneto, Prog. Theor. Phys. **46**, 411 (1970).
[3] O. Penrose and L. Onsager, Phys. Rev. **104**, 576 (1956).
[4] A. Andreev and I. Lifshitz, Sov. Phys. JETP **29**, 1107 (1969).
[5] G. V. Chester, Phys. Rev. A **2**, 256 (1970).
[6] R. A. Guyer, Phys. Rev. Lett. **26**, 174 (1971).
[7] M. Meisel, Physica B **178**, 121 (1992).
[8] P. Ho, I. Bindloss, and J. Goodkind, J. Low Temp. Phys. **109**, 409 (1997).
[9] E. Kim and M. Chan, Nature (London) **427**, 225 (2004).
[10] E. Kim and M. Chan, Science **305**, 1941 (2004).
[11] E. Kim and M. Chan, J. Low Temp. Phys. **138**, 859 (2005).
[12] E. Kim and M. H. W. Chan, Phys. Rev. Lett. **97**, 115302 (2006).
[13] A. Penzev, Y. Yasuta, and M. Kubota, J. Low Temp. Phys. **148**, 677 (2007).
[14] M. Kondo, S. Takada, Y. Shibayama, and K. Shirahama, J. Low Temp. Phys. **148**, 695 (2007).
[15] Ann Sophie C. Rittner and J. D. Reppy, Phys. Rev. Lett. **98**, 175302 (2007).
[16] Y. Aoki, J. C. Graves, and H. Kojima, Phys. Rev. Lett. **99**, 015301 (2007).
[17] J. Day and J. Beamish, Nature (London) **450**, 853 (2007).
[18] D. S. Greywall, Phys. Rev. B **16**, 1291 (1977).
[19] J. Day, T. Herman, and J. Beamish, Phys. Rev. Lett. **95**, 035301 (2005).
[20] J. Day and J. Beamish, Phys. Rev. Lett. **96**, 105304 (2006).
[21] A. Rittner, W. Choi, E. J. Mueller, and J. Reppy, arXiv:0904.2640 (unpublished).
[22] G. Bonfait, H. Godfrin, and B. Castaing, J. Phys. (France) **50**, 1997 (1989).
[23] S. Sasaki, R. Ishiguro, F. Caupin, H. Maris, and S. Balibar, Science **313**, 1098 (2006).
[24] S. Sasaki, F. Caupin, and S. Balibar, Phys. Rev. Lett. **99**, 205302 (2007).
[25] S. Sasaki, F. Caupin, and S. Balibar, J. Low Temp. Phys. **153**, 43 (2008).
[26] M. Boninsegni, A. B. Kuklov, L. Pollet, N. V. Prokof'ev, B. V. Svistunov, and M. Troyer, Phys. Rev. Lett. **97**, 080401 (2006).
[27] N. Prokof'ev and B. Svistunov, Phys. Rev. Lett. **94**, 155302 (2005).
[28] D. M. Ceperley and B. Bernu, Phys. Rev. Lett. **93**, 155303 (2004).
[29] B. K. Clark and D. M. Ceperley, Phys. Rev. Lett. **96**, 105302 (2006).
[30] L. Pollet, M. Boninsegni, A. B. Kuklov, N. V. Prokof'ev, B. V. Svistunov, and M. Troyer, Phys. Rev. Lett. **98**, 135301 (2007).
[31] M. Boninsegni, A. B. Kuklov, L. Pollet, N. V. Prokof'ev, B. V. Svistunov, and M. Troyer, Phys. Rev. Lett. **99**, 035301 (2007).
[32] Z. Nussinov, A. V. Balatsky, M. J. Graf, and S. A. Trugman, Phys. Rev. B **76**, 014530 (2007).
[33] A. Andreev, JETP Lett. **85**, 585 (2007).
[34] G. Biroli, C. Chamon, and F. Zamponi, Phys. Rev. B **78**, 224306 (2008).
[35] M. Boninsegni, N. Prokof'ev, and B. Svistunov, Phys. Rev. Lett. **96**, 105301 (2006).
[36] M. W. Ray and R. B. Hallock, Phys. Rev. Lett. **100**, 235301 (2008).
[37] M. W. Ray and R. B. Hallock, J. Phys.: Conf. Ser. **150**, 032087 (2009).
[38] J. R. Beamish, A. Hikata, L. Tell, and C. Elbaum, Phys. Rev. Lett. **50**, 425 (1983).
[39] C. Lie-zhao, D. F. Brewer, C. Girit, E. N. Smith, and J. D. Reppy, Phys. Rev. B **33**, 106 (1986).
[40] E. Adams, Y. Tang, K. Uhlig, and G. Haas, J. Low Temp. Phys. **66**, 85 (1987).
[41] G. C. Straty and E. E. Adams, Rev. Sci. Instrum. **40**, 1393 (1969).
[42] M. F. Wilson, D. O. Edwards, and J. T. Tough, Rev. Sci. Instrum. **39**, 134 (1968).
[43] J. Beamish (private communication).
[44] J. Reppy (private communication).
[45] F. Pobell, *Matter and Methods at Low Temperatures* (Springer, New York, 1996).
[46] N. Mikhin, A. Polev, E. Rudavskii, and Y. Vekhov, J. Low Temp. Phys. **148**, 707 (2007).
[47] M. W. Ray and R. B. Hallock, J. Phys.: Conf. Ser. **150**, 032088 (2009).
[48] N. Ford, R. B. Hallock, and K. Langley, J. Low Temp. Phys. **148**, 653 (2007).
[49] H. Suzuki, J. Phys. Soc. Jpn. **35**, 1472 (1973).
[50] S. Balibar and F. Caupin, Phys. Rev. Lett. **101**, 189601 (2008).
[51] M. W. Ray and R. B. Hallock, Phys. Rev. Lett. **101**, 189602 (2008).
[52] S. Harrison and K. Mendelssohn, *Low Temperature Physics* (Plenum, New York, 1974), Vol. 1, p. 298.